

Configuration Dependence of Pressure Driven Modes in Heliotron Plasmas

S. Sakakibara, K.Y. Watanabe, H. Yamada, S. Ohdachi, Y. Suzuki, H. Funaba, Y. Narushima, F. Watanabe, K. Toi, K. Ida, I. Yamada, K. Narihara, K. Tanaka, T. Tokuzawa and LHD Experimental Group

National Institute for Fusion Science, 322-6 Oroshi-cho, Toki 509-5292, Japan

This article describes experimental results on finding the onset parameters of the low- m MHD modes and the parameter dependence of the amplitude in the Large Helical Device. The control of peripheral pressure gradients with the gas-puff modulation technique was done in the plasmas with different magnetic Reynolds number S . The $m/n = 1/1$ mode excited in the periphery appeared when the pressure gradient on the resonance exceeded the critical value. The critical pressure gradient for the mode-onset is almost the same even in different S plasmas. Also it was found that the mode was enhanced clearly with the decrease in S under the condition with the same pressure gradient and magnetic configurations. These results contribute to verify the validity of the linear MHD stability.

Keywords: Large Helical Device, Heliotron Configuration, MHD Instability, Interchange Mode, Magnetic Reynolds Number

1. Introduction

An understanding of characteristics of pressure driven modes is one of the major issues for high-beta plasma production in magnetic confinement systems. Experimental characterization of ideal/resistive interchange instability has been required for clarifying the validity of theoretical prediction on linear stability boundary, which contributes the extension of free degree of configuration optimization in stellarators and heliotrons. In Large Helical Device (LHD), experimental studies on ideal and resistive instabilities by making a use of wide free degree of magnetic configurations are possible, and we have investigated them focusing on the effect of MHD activity on the plasma profile and confinement [1-4]. The experimental results suggest that MHD activities near ideal stability boundary affect the plasma profile and sometimes lead to the minor collapse, whereas they never grow as large as that causing the disruption in tokamaks [5]. It has been predicted that the resistive modes are unstable even in the low-beta plasmas and enhanced with beta value, while the growth of the mode is stopped immediately and the effect on the confinements seems to be weak in the beta range of 5 % [6].

The findings of the onset and saturation level of the mode are suitable for characterization of the instability. We have proceeded to construct the database on the above parameters of magnetic fluctuations observed in several machines in order to find the common understanding of MHD activity in stellarators and heliotrons [7]. Regarding the saturation level of the mode, the amplitude has clear

dependence of the magnetic Reynolds number S , and the dependence is close to that of the linear growth rate of the resistive interchange mode [5]. This tendency can be seen in different machines with different S plasmas [1]. On the other hand, we made the experiments for controlling edge pressure gradient using movable limiter in order to find the onset of the mode [8]. The peripheral modes disappeared one after another when the limiter was inserted, and we found the S and D_R at the onset of each mode, where D_R is the index of the stability boundary of the resistive interchange mode. The results were consistent within a factor of two with theoretical prediction [8].

Here we report the experimental results of pressure gradient control using the gas-puff modulation technique in order to clarify the effects of pressure gradient and S on the onset of MHD mode. The active control of the pressure gradient is useful to find the onset-parameters because the peripheral MHD modes appear in the beginning of discharge, which means difficulty in identifying the mode-onset in the quasi-steady-state plasmas. The edge pressure (and the pressure gradient) was changed by the increase and decrease in gas-fueling in the different S plasmas. Here we focus on the behavior of the $m/n = 1/1$ mode which is excited in the periphery with magnetic hill.

2. Experimental Condition

The LHD is the heliotron device with a pair of continuous helical coils and three pairs of poloidal coils and all of coils are superconductive. The magnetic axis position R_{ax} can be changed from 3.4 to 4.1 m by controlling poloidal coil currents, whereas plasma aspect

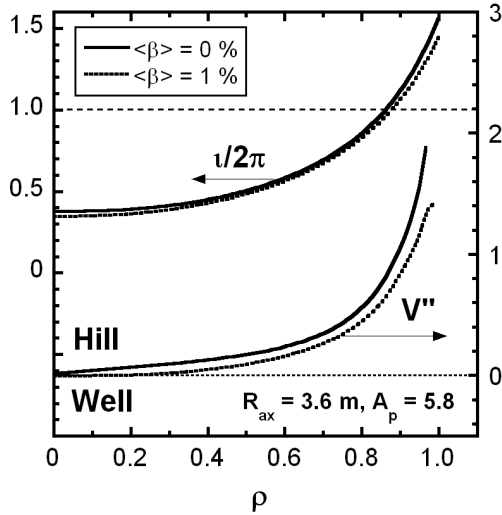


Fig.1 Rotational transform and V'' profiles at the configuration with $R_{ax} = 3.6$ m and $A_p = 5.8$.

ratio A_p can be selected from 5.8 to 8.3. The configuration with R_{ax} of 3.6 m and $A_p = 5.8$ was applied for this experiments, which is the standard configuration in LHD. The toroidal magnetic field B_t was set at 1, 1.5 and 2 T for changing S .

Figure 1 shows the typical profiles of rotational transform and V'' in the plasmas with $\langle\beta\rangle = 0$ and 1 %, respectively, where V denotes the volume encircled by the magnetic surface. The positive and negative V'' regimes correspond to the magnetic hill and well, respectively. These profiles are calculated by 3D MHD equilibrium code VMEC under the currentless condition. The pressure profile was assumed as $P_0(1-\rho^2)(1-\rho^8)$, which is close to an actual profile in the low-beta plasma. The rotational transform profile slightly changes due to finite-beta effects, while the location of the $t/2\pi = 1$ resonant surface at which $m/n = 1/1$ mode is excited almost remains at around ρ of 0.9. The V'' decreases with the beta value due to the outward shift of the magnetic axis, whereas there is still magnetic hill, especially, in the periphery. The D_R at the $t/2\pi = 1$ resonance increases with the beta value and the pressure gradient, and approaches 0.1 when the $\langle\beta\rangle$ is around 1 %. Ideal interchange mode in the periphery is stable in this experiment.

Electron density is controlled by Hydrogen gas-puff. Electron temperature and density profiles were measured with Thomson scattering system and FIR interferometer, respectively. For identifying characteristics of MHD modes, 22 magnetic probes were applied mainly.

3. Gas Puff Modulation Experiments

Figure 2 shows the example discharge with modulating H_2 gas-fueling in the configuration with $B_t =$

1.5 T. The co- and counter neutral beams (NB) were applied here and the each input power is 1.3 and 2.5 MW, respectively. The NB's were injected from 0.3 s, and co-NB was turned off at 2.02 s. The gas-puff was applied from 0.7 s and started to decrease at 0.9 s, and then line-averaged electron density \bar{n}_e and the volume averaged beta value $\langle\beta_{dia}\rangle$ started to increase and oscillated between 0.8 % and 1 %. The central electron temperature T_{e0} is about 2 keV at 0.9 s and decreased stepwise when the \bar{n}_e increased. The magnetic fluctuation with up to 50 kHz was enhanced with the increase in \bar{n}_e . The several MHD modes such as $m/n = 1/1, 2/3, 3/4, 4/5$ and $4/6$ were observed as shown in the bottom figure, where m and n are poloidal and toroidal mode numbers, respectively. These modes nominally rotated in the electron-diamagnetic direction and are expected to be located in the periphery as predicted from Fig.1, if they are resonant modes. While the $m/n = 1/1$ mode appeared when the \bar{n}_e and $\langle\beta_{dia}\rangle$ were increased, it disappeared with the decreases in the \bar{n}_e and $\langle\beta_{dia}\rangle$. The frequencies of other modes were oscillated with \bar{n}_e and T_e , which is predicted to be due to the change of the rotation of the bulk plasma with gas-puff modulation. The modes except for $m/n = 1/1$ one were continuously observed. The plasma current I_p decreasing the rotational transform gradually increases with time and reached about 15 kA at the end of the discharge. The current is mainly driven by NB because of unbalanced injection of NB. The central rotational transform is decreased to 0.03 when the I_p is

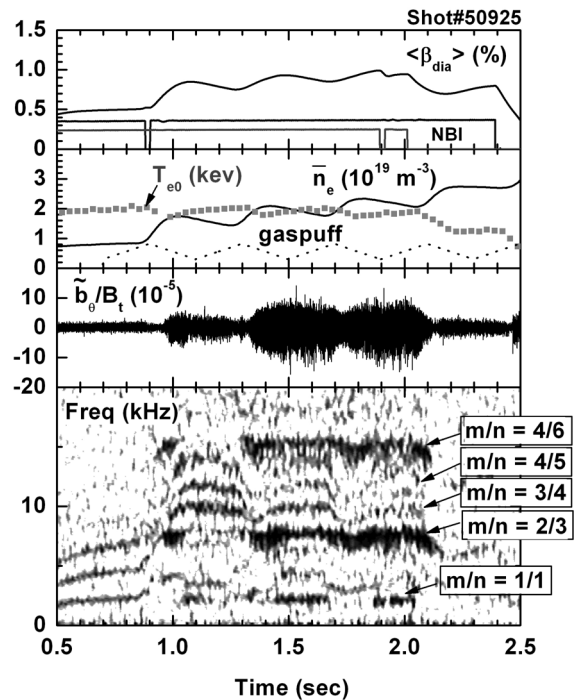


Fig.2 MHD activities in the Discharge with modulating gas-fueling in the configuration with $R_{ax} = 3.6$ m and $B_t = 1.5$ T.

15kA and has the parabolic profile, which hardly affects the stability property in the periphery.

The gas puff modulation experiments were done in the different B_t configuration in order to change the S . Figure 3 shows the temporal changes of S , the beta gradient $d\beta/dr$ at the $i/2\pi = 1$ resonance and the $m/n = 1/1$ mode in the configurations with 2, 1.5 and 1 T. The perturbations of the S and $d\beta/dr$ due to the gas modulation in the $B_t = 2$ T case is relatively smaller than the other cases because the modulation speed is relatively high compared with the fig.3 (b) and (c) cases. The $\langle\beta_{dia}\rangle$ was set to 0.8 ~ 1.3 % at any configurations. The $d\beta/dr$ was increased and decreased with the increase and decrease in gas-fueling. The $m/n = 1/1$ mode appeared at around when the $d\beta/dr$ exceeded 3~ 4 %/m at $B_t = 2$ and 1.5 T cases, whereas the mode was continuously observed appear above the critical value of the $d\beta/dr$ as shown in Fig.3 (c). The onset seems to strongly depend on the $d\beta/dr$ rather than S . On the other hand, the mode was enhanced with the decrease in S rather than the increase and the decrease of $d\beta/dr$. The changes of the amplitude of the mode were summarized in Fig.4. The data in the steady state plasmas

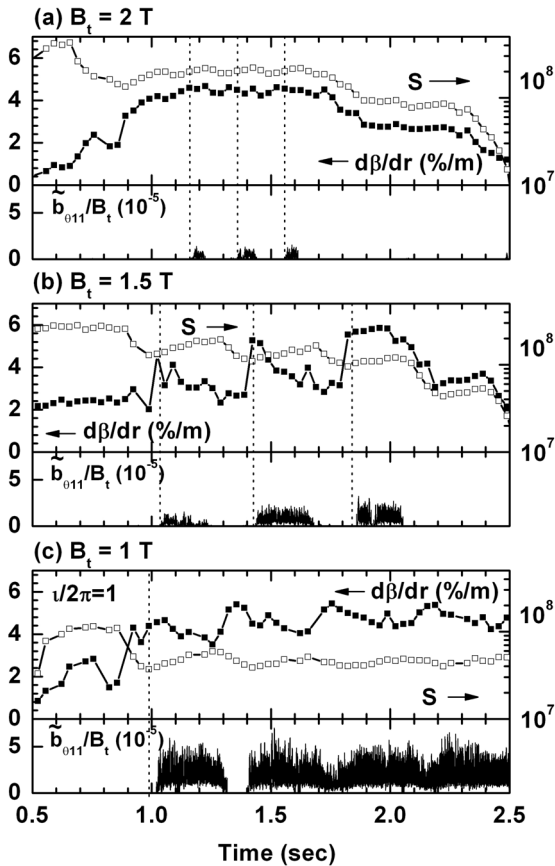


Fig.3 Temporal changes of magnetic Reynolds number, beta gradient at the $i/2\pi = 1$ magnetic surface and $m/n = 1/1$ mode in the configuration with (a) 2 T, (b) 1.5 T and (c) 1 T.

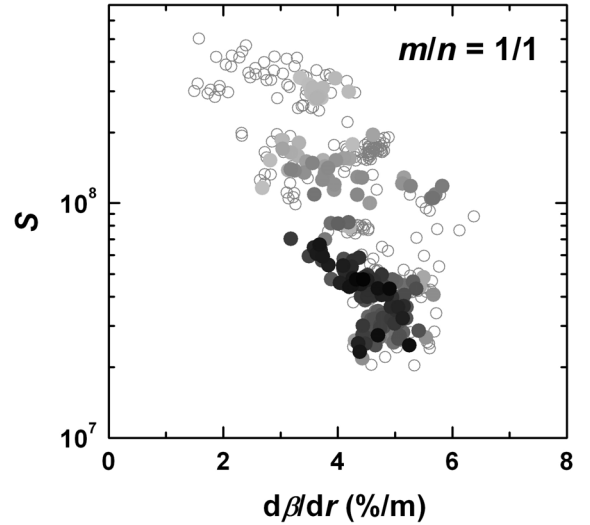


Fig.4 The amplitude of the $m/n = 1/1$ mode in the S and $d\beta/dr$ diagram. The open circle denotes no observation of the $m/n = 1/1$ mode, and the closed circle corresponds to the root mean square of the amplitude of the mode during 10 ms. The change of the color of the closed circle from gray to black corresponds to $b_\theta/B_t = 1 \times 10^{-6}$ to 3×10^{-5} .

of 12 discharges was applied here. The amplitude of the mode was increased with the decrease in S at the constant $d\beta/dr$. This tendency is consistent with the previous study on high-beta plasma [5].

4. Discussion and Summary

The relationship between the mode property and the parameters related with the resistive interchange mode, the beta gradient and magnetic Reynolds number, has been investigated in the low-beta plasmas through the experiments with gas puff modulation. The plasmas were situated in ideal-stable and resistive-unstable regimes. According to the linear theory on the resistive interchange mode, the growth rate increases with D_R with the beta gradient as the driving term, and with the reduction of the magnetic Reynolds number [9]. Therefore, we speculate that the stability boundary which corresponds to ‘mode-onset’ has the same dependence. Regarding the amplitude of the mode, it strongly depends on the magnetic Reynolds number, and the mode was stabilized in the high- S region even under the condition that the beta gradient is constant as shown in Fig.4. The mode onset seems to depend on the beta gradient rather than magnetic Reynolds number, however, the analyses in the wider range of the beta gradient are required for clarifying the relation with their dependences. For example, the regime with lower beta gradient and lower magnetic Reynolds number should be investigated.

The significance of the linear stability boundary,

especially, of the resistive interchange mode, should be clarified experimentally because the mode is predicted to be unstable even in the low-beta plasma of the heliotron configuration despite several low-order resonances are located in the most unstable region. It has been found experimentally that their modes have the weak effect on the profile and the global confinement in the present beta range with up to 5%. However, there is the possibility that the island overlap due to their modes affect the property of the plasma confinement and the magnetic topology in the higher beta range. Therefore, the experiments for the identification of the mode-onset are important to verify the validity of the stability prediction.

Acknowledgements

This work is supported by NIFS under contract No.NIFS05ULHH517.

- [1] S. Sakakibara *et al.*, Nucl. Fusion **41**, 1177 (2001).
- [2] S. Sakakibara *et al.*, Plasma Phys. Control. Fusion **44**, A217 (2002).
- [3] K.Y. Watanabe *et al.*, Nucl. Fusion **45**, 1247 (2005).
- [4] S. Sakakibara *et al.*, Plasma Fusion Res. 1, 003 (2006).
- [5] S. Sakakibara *et al.*, Fusion Science and Technol. **50**, 177 (2006).
- [6] K.Y. Watanabe *et al.*, this conference.
- [7] A. Weller *et al.*, this conference.
- [8] S. Sakakibara *et al.*, Plasma Fusion Res. 1, 049 (2006).
- [9] K. Ichiguchi *et al.*, Nucl. Fusion **29**, 2093 (1989).